

Design of an Optimized Charge-Blended Energy Management Strategy for a Plugin Hybrid Vehicle

Ravi Shankar

Automotive Mechatronics Centre
Dep. of Automotive Engineering
School of Engineering
Cranfield University, UK
r.shankar@cranfield.ac.uk

Dr James Marco

Automotive Mechatronics Centre
Dep. of Automotive Engineering
School of Engineering
Cranfield University, UK
j.marco@cranfield.ac.uk

Prof Francis Assadian

Automotive Mechatronics Centre
Dep. of Automotive Engineering
School of Engineering
Cranfield University, UK
f.assadian@cranfield.ac.uk

Abstract - This paper introduces the design of a charge blended energy management control system for use within a plugin hybrid electric vehicle. The approach taken extends the local cost function optimization routine associated with an Equivalent Fuel Consumption Method (EFCM) in which the charge-sustaining penalty factor is calculated online from an integrated PI controller rather than being derived from a pre-calibrated lookup table. The performance of the controller for a hybrid vehicle exercised over a number of different drive-cycles is presented. The powertrain model used to design and evaluate the system is derived from data logged onboard a number of different electric vehicles under real-world driving conditions.

Plugin Hybrid Electric Vehicle (PHEV), Energy Management, Equivalent Fuel Consumption Method (EFCM), Controller Optimization

I. INTRODUCTION

Within the automotive and road transport sector, one of the main drivers for technological development and innovation is the need to reduce the vehicle's fuel consumption and the emission of Carbon Dioxide (CO₂) [1]. Legislative requirements are motivating manufacturers and subsystem suppliers to develop new and innovative electric vehicles (EV) and hybrid electric vehicles (HEV) concepts. In recent years, plug-in hybrids (PHEV) have also attracted considerable interest from both academia and industry.

A PHEV will typically have two primary modes of operation, namely a charge depleting mode (CD) and a charge sustaining mode (CS). Within a CD mode the vehicle operates as a zero emissions vehicle and the battery is depleted until it reaches a lower threshold. Conversely within a CS mode, an internal combustion engine (ICE), or equivalent is used to maintain the battery state of charge (SoC) within the required range. For a given journey that exceeds the zero emissions range of the vehicle, a number of publications describe a PHEV operating initially in its CD mode until the battery has depleted and then transitioning to the CS mode until the vehicle has reached its destination. Research published in [2] advocates a third mode of operation, the charge blended (CB) mode in which both the ICE and the electrical subsystems are optimally used throughout the entire journey. Because the ICE is able to

operate in its most efficient region for comparatively longer, simulation results presented in [2] demonstrate an overall reduction in CO₂ for the journey.

The aim of this paper is to design and evaluate a CB energy management strategy for a PHEV. The instantaneous power split between the electrical subsystems and the ICE is calculated using the established Equivalent Fuel Consumption Method (EFCM) of local cost function optimization. However, the EFCM is extended by means of integrating it with a Proportional plus Integral (PI) controller in order to obtain the required SoC trajectory for the high voltage (HV) battery throughout the trip. In order to benchmark the performance of this new approach, the resulting powertrain efficiency is compared against that achieved from both a conventional EFCM controller and a thermostat strategy in which the ICE is only activate during the CS mode of vehicle operation.

This paper is structured as follows; Section II describes the derivation of the PHEV plant model employed as the foundation of this study. Sections III and IV present the design of the different energy management control systems for the PHEV. Section V describes the method of comparison used to simulate and evaluate the different control systems. Section VI presents the Results and Discussion. Conclusions and Further work are discussed in Section VII.

II. DEVELOPMENT OF THE PHEV POWERTRAIN MODEL

A. Model Aims and Structure

In order to support the evaluation of the different energy management techniques, a powertrain model for the PHEV is required of appropriate fidelity to facilitate vehicle simulations over the different drive-cycles. With simulation times in excess of 2000 seconds, a pseudo steady-state model is required in which the primary elements of the powertrain are represented by their non-linear efficiency characteristics. The powertrain model is designed to be an *enhanced* backward-facing model. Power calculations *flow* from the wheels to the main system components. However, forward-facing constraints are imposed to ensure that none of the component power ratings are invalidated. The simulation terminates if the required velocity trace cannot be met.

B. Data Source

Parameterization of the electrical subsystems is based on the real-world vehicle usage data obtained from the Smart Move 2 Electric Vehicle Trail. As part of this program, 7 Smart Electric Drives (Smart EDs) were employed as the test vehicles. A full description of the vehicle trail is provided in [3] and will therefore not be repeated here. Over the course of 4268 km of driving, values of battery current (i_b), battery terminal voltage (v_t), vehicle speed (v) and inverter current (i_m) were recorded from the vehicle's Controller Area Network or CAN bus. As presented below, this data forms the basis for the derivation of the efficiency maps for both the electrical machine and HV battery. The remainder of this section describes the three main elements of the PHEV powertrain model, namely the vehicle mass, the electrical architecture and the ICE.

C. Vehicle Mass

A vehicle coast down curve was experimentally obtained for the Smart ED. The coast down curve defines the resistive force (F_r) within the powertrain as a function of vehicle speed. The equation below defines the 3rd order polynomial best-fit approximation to the test data. The final term of 146.8 N represents the tire rolling resistance of the vehicle. The slope of the terrain (α) during the test was calculated using the measured height data obtained from the onboard GPS.

$$F_r = (8 \times 10^{-5})v^3 + (0.0241)v^2 + (0.1456)v + 146.8 \cos(\alpha) \quad (1)$$

The associated wheel power (P_w) for the vehicle is given below:

$$P_w = M_v \frac{dv}{dt} + F_r + \sin(\alpha) \quad (2)$$

The mass of the vehicle (M_v) was measured as 1036 kg.

D. Electrical Architecture

1) Electrical Machine Model and Efficiency

The Smart ED employs a 50 kW brushless DC machine. For the PHEV model, the electric machine and the associated inverter have been considered as a single integrated system. Equation (3) was employed to calculate the efficiency of the electrical drive system (η_e):

$$\eta_e = \frac{P_w}{v_t i_b} \quad (3)$$

The values of v_t and i_b were recorded during the EV evaluation trail under a number of different driving conditions [3]. Fig.1 shows the mean efficiency for the electrical machine as a function of both shaft torque (τ_m) and rotor velocity (ω_m).

2) Battery Model and Efficiency

The Smart ED employs a 16.5kWh Lithium Ion battery, with a peak power rating of 30kW during discharge and 10kW for charge. A steady-state, equivalent circuit model is employed to represent the efficiency of the HV battery. This method is widely reported within the literature [4]. Fig.2

presents the circuit, which comprises of a controlled open circuit voltage (v_{oc}) in series with a non-linear variable resistance (R).

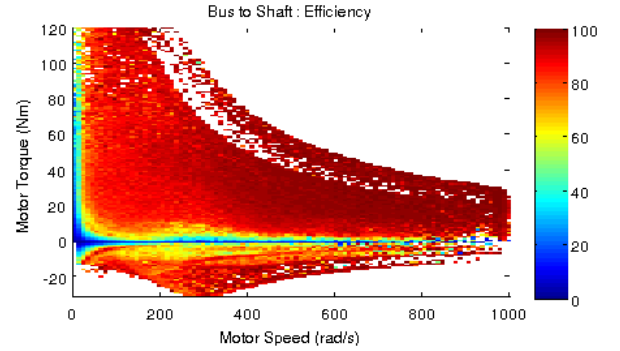


Fig. 1: Measured efficiency of the electrical drive system

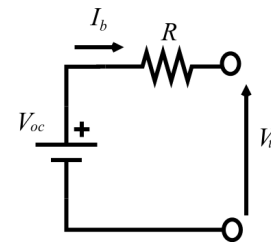


Fig. 2: Battery model

The value of v_{oc} was estimated using the data recorded from [3]. The data was analyzed and the points in which i_b is zero were noted. Under these conditions $v_{oc} = v_t$. Fig.3 shows the results of this exercise and presents the estimated v_{oc} as a function of measured pack temperature and recorded SoC. From Figs. 2 and 3, it is possible to derive an expression for the efficiency of the HV battery (η_b):

$$\eta_b = \frac{v_{ocv} i_b}{v_t i_b} \quad (4)$$

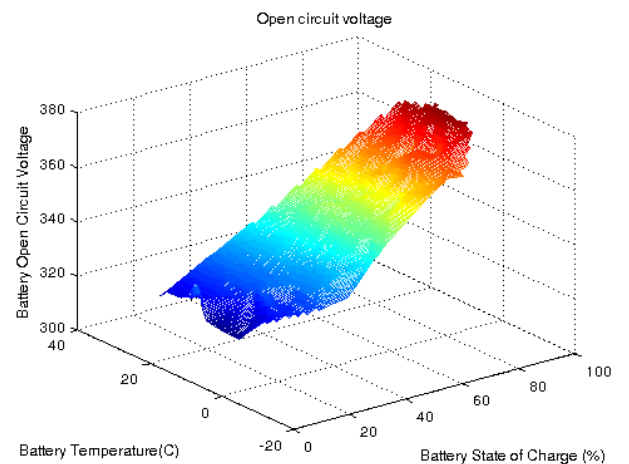


Fig. 3: Estimated battery open circuit voltage

As reported in [5] above 20% SoC, the internal resistance of lithium cells is largely insensitive to variations in battery SoC. However, battery efficiency does vary considerably due to changes in ambient temperature. Fig. 4 presents the efficiency of the battery system as a function of battery current and SoC. For the purpose of this study, battery pack temperature was assumed constant at 20 °C.

E. The ICE Model and Efficiency

When considering the design of an ICE model there are various levels of possible fidelity. As reported in [6], for a backward facing model in which the emphasis is on fuel economy estimation rather than transient load prediction, the ICE is often represented as a steady-state look-up table. This map defines the instantaneous mass flow rate of fuel and Best Specific Fuel Consumption (BSFC) line for the ICE. Fig. 5 presents the engine BSFC map employed within this study. The map defines the steady-state performance for a 0.7 liter naturally aspirated 4 cylinder spark ignition engine with a maximum power of 46kW. The characteristics of this ICE are typical of the low power ICE variants often employed as a “range-extender” or Auxiliary Power Unit (APU) within a PHEV.

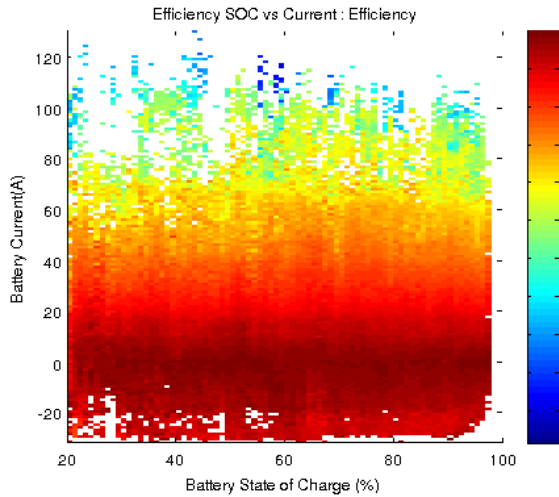


Fig. 4: Estimated battery efficiency as a function of SoC

F. Summary of Model Equations

Given the non-linear parameterization data and efficiency characteristics given above, for the battery discharge conditions, equations (5)-(16) summarize the PHEV plant model employed within the control study discussed in the preceding sections.

Based on the input drive-cycle, the wheel power (P_w) can be calculated directly from (1) and (2). Taking into account the efficiency of the electrical drive system including the efficiency of the final drive, the power on the HV bus can be calculated as follows:

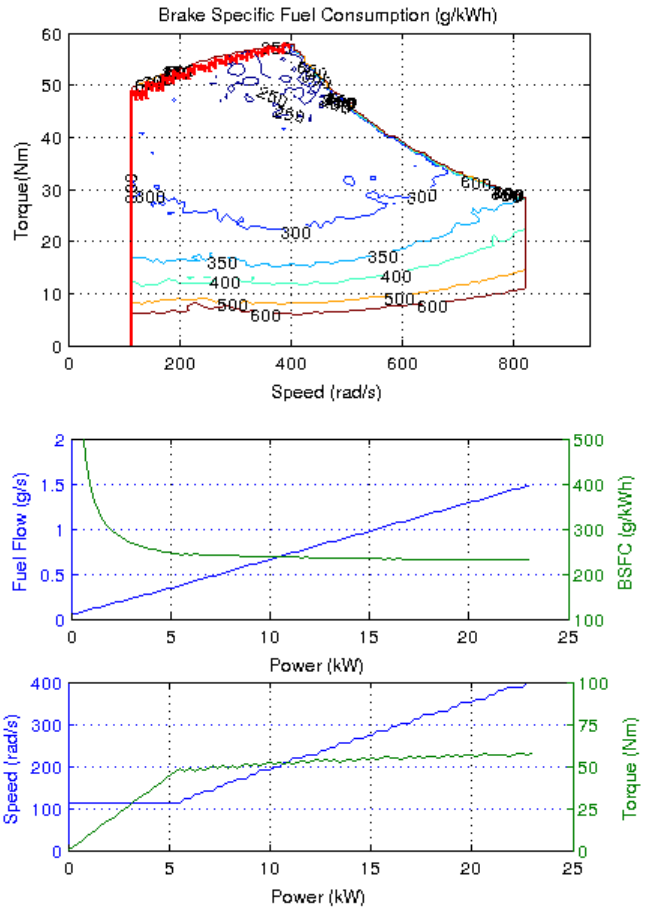


Fig. 5: Engine and Generator.

(a) Brake Specific Fuel Consumption Map (b) Best Fuel Consumption Operation Line (c) Target for engine controller

$$P_B = \frac{P_w}{\eta_e} \quad (5)$$

$$\eta_e = f^n(\tau_m, \omega_m) \quad (6)$$

$$\tau_m = F_r r_w \quad (7)$$

$$\omega_m = \frac{v}{r_w} \quad (8)$$

The term r_w defines the rolling radius of the wheel. All other parameters are as previously defined. Given the power on the HV bus, the total battery power can be calculated as follows:

$$P_{Bat} = P_B + P_{aux} + P_{ICE} \quad (9)$$

The term P_{aux} defines an average auxiliary power demand for the vehicle and P_{ICE} the power contribution from the ICE. Given P_{Bat} , it is possible to calculate the required values of battery current (i_b) and battery SoC:

$$i_b(t-1) = \frac{P_{Bat}}{v_t(t-1)} \quad (10)$$

$$v_{oc} = f^n(SoC, T) \quad (11)$$

$$SoC = SoC_{ic} - \frac{1}{3600Q} \int_{t=0}^{t=STOP} i_b dt \quad (12)$$

$$i_b = \frac{v_{oc} - v_t}{R_{Bat}} \quad (13)$$

$$v_t = v_{oc} - i_b R_{Bat} \quad (14)$$

where Q defines the manufacturers rated battery capacity, R_{Bat} defines the equivalent value of battery internal resistance derived from Fig. 4, t represents simulation time and finally, SoC_{ic} the initial conditions for the battery SoC at the start of the simulation. All other parameters are as previously defined.

The required power from the ICE is a function of the energy management strategy and will be discussed in the following Section. With respect to Fig. 5, given P_{ICE} , the instantaneous mass flow rate of fuel (g) and the total fuel consumed over the cycle (g_{total}) can be calculated as shown below:

$$g = f^n(P_{ICE}) \quad (15)$$

$$g_{total} = \int_{t=0}^{t=stop} g dt \quad (16)$$

Numerical simulations and validation of the above model is provided in [5] and will therefore not be repeated again here.

III. DESIGN OF A THERMOSTATE ENERGY MANAGEMENT STRATEGY

When designing a thermostat energy management strategy, there is relatively little analytical work that can be undertaken. The lower and upper thresholds for the strategy are defined that determine when the ICE / APU is switched on to replenish battery SoC and turned off respectively. Additional rules are often added to the heuristic control system to prevent the APU from rapidly switching, thereby causing unwanted noise, vibration and harshness (NVH) or driveability concerns within the vehicle. For the purpose of this study a simple thermostat strategy is employed in which the upper and lower SoC thresholds are defined in addition to a hysteresis function to prevent excessive cycling of the APU.

Within industry, much of the effort when integrating a thermostat approach relates to the calibration of the upper threshold. The significance of this parameter for achieving a low value of CO₂ is discussed further in Section VI. Fig. 6 presents the sensitivity for the final CO₂ output of the PHEV over the New European Drive-Cycle (NEDC), for a lower threshold of 25% SoC to a range of different upper thresholds. Since there is an inherent coupling between the physical size of the energy storage medium, the useable SoC range and the characteristics of the journey profile (distance or kWh demand) the final CO₂ is highly variable and non-deterministic.

For the purpose of this study, two calibrations for the thermostat controller have been employed; the first relates to a strategy that has been optimized for use over the NEDC. The second, relates to a modified calibration that is optimized for each route under investigation. Fig. 6, shows the controller calibration options for a controller tuned specifically to achieve the best Tank to Wheel (TTW) emissions from the vehicle over the legislative, NEDC, drive-cycle.

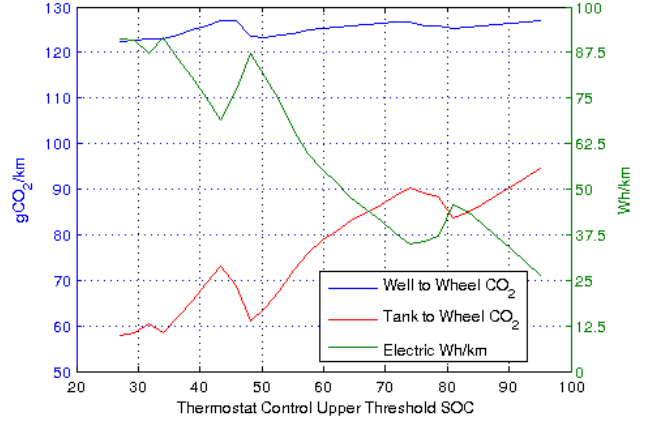


Fig. 6: Calibration of the thermostat controller (lower SoC threshold set to 25%)

IV. DESIGN OF A EFCM ENERGY MANAGEMENT STRATEGY

The EFCM is a real-time, local optimization technique that was first proposed in [8] and has been subsequently refined and extended in a number of further publications, for example [7]. The technique has also been applied to a wide range of different HEV powertrain architectures, each employing different degrees of hybridization and subsystem technologies.

A. Derivation of the EFCM Strategy

The aim of this section is to present the structure, cost function and constraints associated with the proposed EFCM.

The primary function of the energy management controller is to ascertain the optimized value of P_{ICE} . For a given value of P_B , at each time-step, the strategy calculates the power demands to be sent to both the ICE and the electrical machine:

$$\begin{aligned} P_{ICE} &= (\beta) P_B \\ P_m &= (1-\beta) P_B \end{aligned} \quad (17)$$

where β represents the power split ratio. A controller sample rate of 100 ms was selected. Given this constraint, 100 unique values of β are computed for each iteration of the controller. The normalized values of β are calculated such that the following constraints are not invalidated:

$$\begin{aligned} P_{ICE_MIN} &\leq P_{ICE} \leq P_{ICE_MAX} \\ P_m &\leq P_{m_MAX} \\ P_{B_MIN} &\leq P_B \leq P_{B_MAX} \end{aligned} \quad (18)$$

The locally optimized value of β that provides the most efficient power split between the ICE and electrical machine is

calculated at each time-step, by minimizing the following cost function (J):

$$J = MIN(g + g_{equiv} \zeta) \quad (19)$$

where g is calculated from (15), g_{equiv} represents the equivalent fuel consumption of the energy sunk and sourced from the HV battery taking into account the battery efficiency presented in Fig. 4. Finally ζ defines the charge-sustaining penalty function:

$$0 \leq \zeta \leq \zeta_{max} \quad (20)$$

In the majority of published research, ζ represents a static look-up table that is either a linear or sigmoidal function of SoC. For the purpose of this study, two approaches to the definition of ζ have been investigated. The first is to define ζ as a linear function of SoC that weights the use of the electrical subsystems for progressively lower values of SoC (similar approaches have been discussed in [7,9]). The second is to employ a time varying value of $\zeta(t)$, in which the value is calculated from an outer PI control loop. Fig. 7 presents the structure of the integrated PI-EFCM control system.

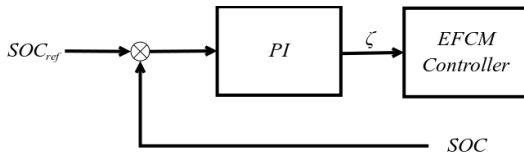


Fig. 7: Integrated PI-EFCM energy management approach

In order for this technique to be successfully applied to a PHEV as part of a CB energy management strategy, the desired set-point trajectory of SoC across the trip (SOC_{ref}) must be known in advance.

V. METHOD OF EVALUATION FOR CONTROL SYSTEM PERFORMANCE

The aim of this Section is to introduce the method of control system evaluation employed within this study. Three drive-cycles have been used; the NEDC, the Artemis cycle and a real-world mixed urban-highway cycle that has been logged as part of the evaluation of the Smart Move 2 trail. The speed profile of this latter cycle is 29.83 km long, it has a top speed of 28 ms⁻¹ and a number of start-stop events. Further information is presented in [3]. For each drive-cycle, four sets of simulations have been undertaken and the CO₂ output of the PHEV recorded for each study:

Study 1: A thermostat controller with an SoC range optimized for each specific cycle under investigation.

Study 2: A thermostat controller with an SoC range of 25 - 34% (i.e.: tuned for the NEDC) used on each cycle.

Study 3: A controller based on the EFCM in which the target SoC is fixed at 25%

Study 4: A controller based on the EFCM and the target SoC is managed across the cycle to facilitate a CB strategy.

In order to draw the final comparisons between a CB strategy and the different forms of a CD-CS strategy, the final energy content of the HV battery is equalized back to the initial SoC value. Using a value of CO₂ equal to 594 gCO₂ / kWh for the UK electrical grid mix, the total CO₂ output of the powertrain can be calculated:

$$CO_2 = CO_2(ICE) + CO_2(grid - kWh) \quad (21)$$

VI. RESULTS AND DISCUSSION

Table 1 presents the CO₂ output for each of the four studies introduced above. For each drive-cycle and control method, the Table shows the overall well-to-wheel (WTW) CO₂ value. In addition, Table 1 also presents how this value is broken down into the corresponding TTW CO₂ and the CO₂ contribution from the electrical supply network. The final SoC of the HV battery is also shown for completeness.

	Study 1	Study 2	Study 3	Study 4
	Thermostat	Thermostat (tuned controller)	EFCM (CS-Mode)	EFCM (CB-Mode)
NEDC				
WTW CO ₂ km ⁻¹	143.47	143.47	143.95	141.87
TTW CO ₂ km ⁻¹	59.87	59.87	58.10	57.30
Whkm ⁻¹	123.10	123.10	127.4	125.48
Final SoC (%)	27.15	27.15	24.81	25.85
ARTEMIS				
WTW CO ₂ km ⁻¹	169.08	168.04	177.13	168.44
TTW CO ₂ km ⁻¹	52.97	48.27	54.76	47.32
Whkm ⁻¹	179.84	188.41	189.87	189.96
Final SoC (%)	28.75	25.65	25.12	25.09
REAL-WORLD ROUTE				
WTW CO ₂ km ⁻¹	123.37	122.36	122.25	121.71
TTW CO ₂ km ⁻¹	59.87	58.00	56.99	56.53
Whkm ⁻¹	89.24	91.25	93.07	93.06
Final SoC (%)	27.86	26.39	25.04	25.04

Table 1: PHEV efficiency results for different energy management techniques

For the real-world drive-cycle, Fig. 8 presents the simulation results from studies 2-4. The figure shows the vehicle speed profile, the instances in which the PHEV is operating as an EV or when additional power is supplied from the ICE. From Table 1, given the variations in the TTW CO₂ values obtained, one of the main drawbacks of the thermostat approach are highlighted. For a PHEV, final CO₂ achieved for the trip or drive-cycle, is highly dependent on the nature of the journey (distance, level of driver demand), the physical size of the battery (kWh) and the upper turn-off threshold for the controller. The ideal calibration for the control system is one that ensures the battery at its lowest allowable SoC point at the end of the journey.

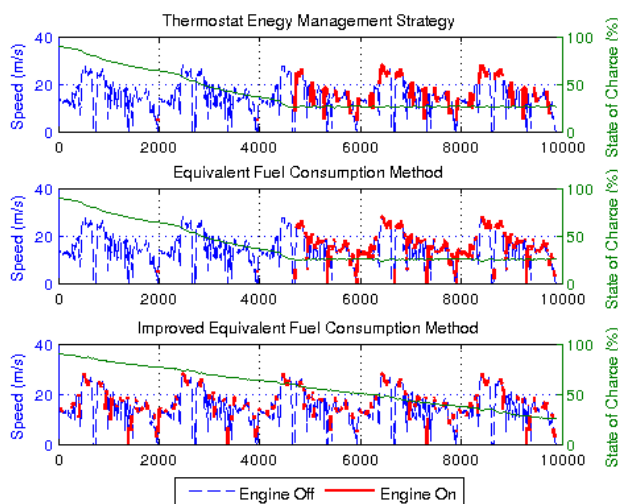


Fig. 8: Drive-cycle results for the PHEV

From Table 1, the primary conclusion that can be drawn is that the CB strategy, designed using an EFCM, consistently results in a PHEV powertrain system with the lowest WTW $\text{CO}_2\text{km}^{-1}$ values. For each cycle, this is true even when compared against a thermostat strategy that has been calibrated to optimize the performance of the vehicle over that cycle. Even though the differences presented here are marginal (in the order of 1-2%) two points should be noted. Firstly, this improvement is achieved simply by adopting a new control methodology. No change to the physical design of the vehicle has been assumed. The second point to note, is that if consideration is restricted to the TTW analysis, then the differential between the different control methods is considerably greater. The CO_2 reduction possibilities are in the order of 4-10%. While the TTW comparisons do not take into account the residual energy content of the HV battery, this method of evaluation is inline with current EU fuel economy measurement processes for PHEVs [10]. Within Regulation 101, two fuel economy metrics are cited, the $\text{CO}_2\text{km}^{-1}$ from the vehicle over the cycle and separately a Whkm^{-1} is also published representing the energy required from the grid to replenish the battery. Currently within the UK only the former is employed when setting vehicle taxation levels and to alleviate congestion charges.

The improvement in efficiency when comparing either a CS or CB control system using EFCM can be seen from Fig. 8. When a closed-loop CB control system is employed, the ICE is consistently used more to support the high power demands from the driver and hence more power is fed directly to the road wheels. With a CS strategy, in which the ICE is used only when the battery SoC has depleted to its lower threshold, the ICE is forced to operate for longer periods within its more inefficient low power regions.

VII. CONCLUSIONS AND FURTHERWORK

A PHEV powertrain model has been developed to support the design and optimization of a CB energy management control system. The electrical subsystems within the model have been calculated from data logged from a Smart ED vehicle under real-world usage conditions.

The energy management technique extends a conventional EFCM controller by integrating it with a closed loop PI control system. The output of the PI controller is a time-varying charge sustaining penalty function that allows for a more robust control of the battery SoC, irrespective of the nature of the drive-cycle or the physical size of the battery.

In order to implement this CB control system, it has been assumed that the control system knows the distance of the journey that the vehicle is traversing. This assumption is valid for a number of applications such as public transportation or vehicle fleet operation. In order to support the wider application of this control method, research is currently ongoing to investigate the accuracy of on-line estimation techniques in which the required SoC trajectory for a CB strategy across a trip can be calculated as a function of the different road types, traffic congestion levels and the differing energy demands from with the driver.

VIII. ACKNOWLEDGEMENTS

The research presented within this paper is supported by the UK Technology Strategy Board (TSB) through the Knowledge Transfer Partnership (KTP) scheme in collaboration with the Morgan Motor Company .

IX. REFERENCES

- [1] C. C. Chan (2002), The state of the art of electric and hybrid vehicles, Proceedings of the IEEE, vol. 90, issue 2, ppP704
- [2] T. Markel, (2005), Energy Storage Systems Considerations for Grid-Charged Hybrid Electric Vehicles, IEEE Conference on Vehicle Power and Propulsion, pp. 62, USA.
- [3] R. Shankar and J. Marco, (2011), Performance of an EV During Real-World Usage, Cenex Hybrid Electric Vehicle Conference, UK.
- [4] O., Tremblay O., et al., (2007), A Generic Battery Model for the Dynamic Simulation of Hybrid Electric Vehicles, IEEE Conference on Vehicle Power and Propulsion, pp. 284, USA.
- [5] R. Shankar, J. Marco and F. Assadian, (2012), A Methodology to Determine Drivetrain Efficiency Based on the External Environment, IEEE Electric Vehicle Conference (IEVC), USA.
- [6] Rizzoni G., L. Guzzella and B. M. Baumann, (1999), Unified Modelling of Hybrid Electric Vehicle Drivetrains, IEEE Transactions on Mechatronics, vol. 4, issue 3, pp. 246-257.
- [7] C. Musardo, G. Rizzoni and B. Staccia, (2005), A-ECMS: An Adaptive Algorithm for Hybrid Electric Vehicle Energy Management, IEEE Conference on Decision and Control, and the European Control Conference, pp. 1816-1823, Spain.
- [8] G. Paganelli, S. Delprat, T. M. Guerra, J. Rimaux and J. J. Santin, (2002), Equivalent Consumption Minimization Strategy for Parallel Hybrid Powertrains, 55th IEEE Vehicular Technology Conference (VTC), vol. 4, pp. 2076-2081, USA.
- [9] G. Paganelli, et al., (2001), General Supervisory Control Policy for the Energy Optimization of Charge-Sustaining Hybrid Electric Vehicles, JSAE, vol. 22, issue 4, pp. 511.
- [10] unece.org, Regulation 101 - Battery Electric Vehicles with Regard to Specific Requirements for Construction and Functional Safety, Last Accessed January, 2011.